

Four-photon excitation of even-parity Rydberg states in krypton and xenon

P. R. Blazewicz,* J. A. D. Stockdale, and J. C. Miller

Chemical Physics Section, Health and Safety Research Division, Oak Ridge National Laboratory, Oak Ridge, Tennessee 37831

T. Efthimiopoulos and C. Fotakis

*Research Center of Crete, P.O. Box 1527, 711 10 Iraklion, Crete, Greece
and Department of Physics, University of Crete, 711 10 Iraklion, Crete, Greece*

(Received 28 August 1986)

Multiphoton ionization via four-photon excitation of high-lying Rydberg states in xenon and krypton has been studied. The p and f series leading to the ${}^2P_{3/2}$ ionization limits as well as the p' and f' autoionizing levels leading to the ${}^2P_{1/2}$ limits have been recorded for both gases. Lower members of the p series in xenon are resolved into $p[\frac{5}{2}]_2$, $p[\frac{3}{2}]_2$, and $p[\frac{1}{2}]_0$ sublevels. Ionization potentials and quantum defects are obtained by a least-squares fitting of the data to the standard Rydberg formula.

INTRODUCTION

The rare gases have served as challenging subjects of study in atomic spectroscopy. They are characterized by a fine-structure splitting in the ion core, ${}^2P_{3/2}$, ${}^2P_{1/2}$, with Rydberg series converging to both states of the ion. This gives rise to a rich autoionizing structure in the energy region between the ionization limits. The spectroscopic challenge of the rare gases is due to the combination of their high ionization limits together with all low-lying singly excited states in a narrow energy region beginning not far below the first limit. Hence, earlier spectroscopic studies of the rare gases consist of vacuum-ultraviolet (vuv) absorption experiments.¹ Selection rules permit the observation of only the s and d states from one-photon absorption from the ground state. The positions of other levels have been determined spectroscopically by emission from gaseous discharges.

Since the rare gases have an ns^2p^6 closed-shell configuration, all lower singly excited states consist of an electron outside of the ion core which has a doublet fine-structure splitting— ${}^2P_{3/2}$, ${}^2P_{1/2}$. The $j-l$ coupling notation is used for the heavier rare gases. States are designated by the label of the orbital containing the excited electron, i.e., when the electron is in the nx orbital ($x = s, p, d, f$), the state is named nx or nx' , primes indicating the states with the ${}^2P_{1/2}$ (higher-energy) core. The spin-plus-orbital angular momentum of the core ($\frac{1}{2}$ or $\frac{3}{2}$) plus the orbital angular momentum of the outer electron couple to give the resultant angular momentum K and coupling with the spin of the outer electron gives the total angular momentum J . States with an electron in an nx orbital are thus labeled $nx[K]_J$ and $nx'[K]_J$.

More recent work in the rare gases has been done by exciting the metastable levels $np^3(n+1)s[\frac{3}{2}]_{J=2}$ or $np^5(n+1)s'[\frac{1}{2}]_{J=0}$ with an electron beam or an electric discharge.²⁻⁸ Stebbings and co-workers²⁻⁴ pioneered the technique in which the large densities of such metastable atoms attainable by electron-beam excitation of an atomic beam easily permit excitation with a laser to higher Rydberg states by a one-photon absorption. This two-step ex-

citation process accesses the even-parity p and f Rydberg states inaccessible in direct one-photon excitation. In this way, Grandin and Husson,⁵ and later, Knight and Wang⁶ have tabulated many members of the $np[\frac{1}{2}]_1$ and $nf[\frac{3}{2}]_1$ Rydberg series in xenon. These and other experiments⁷ have characterized several p' and f' autoionizing levels in xenon, krypton, and argon.

However, many gaps exist in the data. Only a few of the p' and f' levels have been characterized in each atom studied. Furthermore, selection rules allow only one or two J sublevels of each p and f level to be populated from the metastable state.

Intense, tunable, visible, and near-ultraviolet dye lasers permit multiphoton excitation of the states of the rare gases at wavelengths experimentally more tractable than the vuv.^{9,10} More importantly, the different selection rules which operate in multiphoton excitation allow access to states forbidden in one-photon excitation. Thus, the even-parity states not seen in single-photon excitation of the rare gases can be studied using two-photon or four-photon excitation. Since even the lowest excited states in the rare gases are near 10 eV, four-photon excitation is the simplest scheme using available dye lasers. Four laser photons of the same linear polarization can populate $J=0, 2$, and 4 levels from the rare-gas $np^6{}^1S_0$ ground state. Excitation with two beams of crossed polarization can populate the $J=1$ and 3 levels as well. Thus, experiments involving direct multiphoton excitation of ground-state rare-gas atoms appear promising as a way of accessing additional p and f levels.

Recently, Gangopadhyay *et al.*¹¹ using multichannel-quantum-defect theory (MQDT) have calculated large variations in the multiphoton ionization (MPI) cross section for xenon due to autoionizing resonances. The renewed interest in the autoionizing regions as well as our longstanding interest in MPI of rare gases has caused us to reexamine several Rydberg series leading to both limits in krypton and xenon. Here we report the four-photon excitation of members of the p and f Rydberg series leading to the first limits as well as the p' and f' autoionizing series leading to the second limits in xenon and krypton.

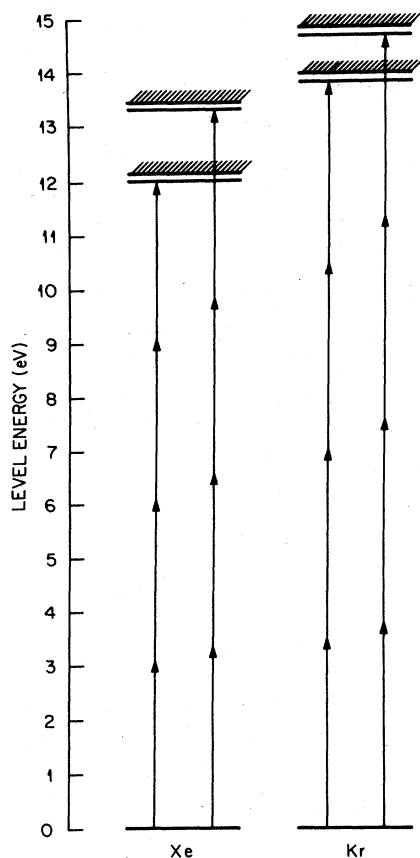


FIG. 1. An energy-level diagram showing direct, four-photon excitation of high Rydberg states in xenon and krypton.

EXPERIMENT

Measurements were made both at Oak Ridge National Laboratory and at the Research Center of Crete. At Oak Ridge, the output of a XeCl excimer laser (308 nm) pumped a pulsed dye laser (Lambda Physik, ~5 mJ/15 ns pulse), the output of which was focused with a 50-mm focal-length lens into a cell containing the rare gas. The dyes used were DPS (410 nm), TMI (375 nm), and DMQ

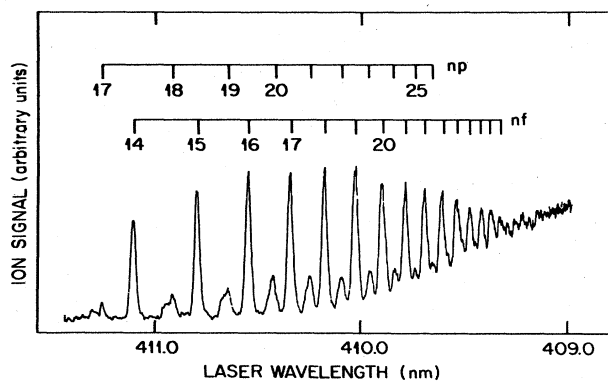


FIG. 2. A multiphoton ionization spectrum showing four-photon excitation of the p and f Rydberg series in xenon.

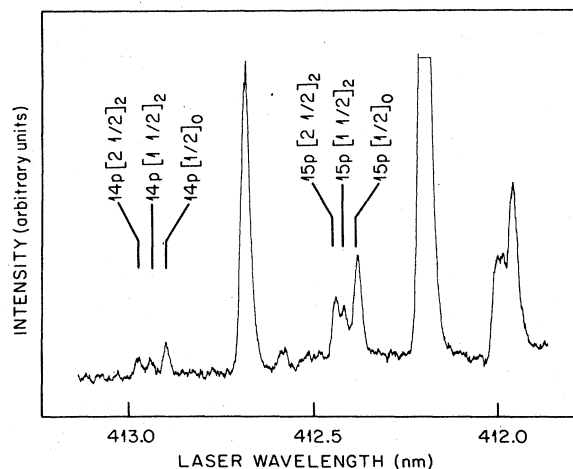


FIG. 3. Several lower members of the p and f Rydberg series in xenon showing resolved p sublevels.

(357 nm). Typical spectra were run at gas pressures of 10–20 Torr. Electrons were collected in a wire-and-cylinder MPI cell and detected with a charge-sensitive preamplifier. Signals were averaged over several laser shots with a boxcar integrator and displayed on an x - y recorder. The bandwidth of the dye laser is 0.01 nm or 0.6 cm^{-1} at 400 nm. The laser wavelength was calibrated from the position of known xenon lines found in each spectral region. The reported line positions are accurate to within 4 cm^{-1} . Spectra are not corrected for variations in dye-laser intensity.

A similar experimental arrangement was employed at the Research Center of Crete. A KrF excimer laser (248 nm) with an output of 100 mJ/pulse was used to pump a Lambda-Physik dye laser. With the dye PTP, output pulses of ~5 mJ/5 ns pulse were obtained over the wavelength region from 344 nm to below the krypton four-photon $^2P_{1/2}$ limit. The bandwidth of this dye laser is 0.2 cm^{-1} . Krypton pressures from less than one Torr to several hundred Torr were used.

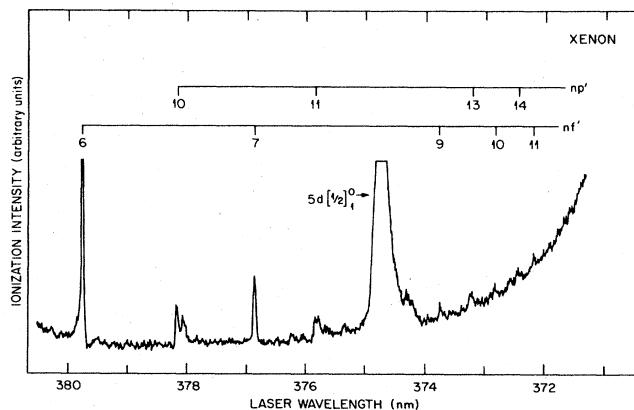


FIG. 4. The np' and nf' autoionizing series in xenon. The tallest features are off the scale of the chart recorder. The larger feature in the middle of the spectrum is a three-photon resonance to the xenon $5d [1/2]_1^0$ level.

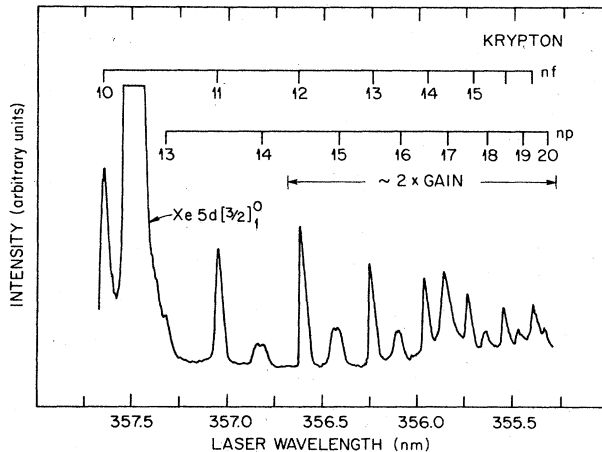


FIG. 5. The p and f Rydberg series in krypton. The right portion of the spectrum is run at increased gain. The largest feature is due to a three-photon resonance in the xenon contaminant, which has a much larger ionization cross section. The rightmost portion of the spectrum includes features from some other contaminant in the cell. The anomalous intensity at the position of the $17p$ is probably due to this.

RESULTS AND DISCUSSION

An energy-level diagram for our experiment is shown in Fig. 1. Four photons from the ground state directly excite Rydberg levels just below each ionization potential (V_{IP}) in xenon and krypton. In general, the first three photons do not match the energy of any intermediate resonance. In some cases as the laser is scanned, three photons do match a lower d resonance. In such cases as the laser is scanned, three photons do match a lower d resonance. In such cases, ionization from the three-photon resonance dominates and obscures the Rydberg structure. Figures 2–6 show the resultant Rydberg series leading to each V_{IP} in xenon and krypton.

Each spectrum consists of a series of sharp, intense f

Rydberg peaks with a much weaker series of p states interleaved. The f resonances consist of the unresolved, overlapping sublevels $nf[1\frac{1}{2}]_2$, $[4\frac{1}{2}]_4$, $[2\frac{1}{2}]_2$, and $[3\frac{1}{2}]_4$. (The f' resonances have only $[3\frac{1}{2}]_4$ and $[2\frac{1}{2}]_2$ components.) As shown in Fig. 3, the lower p states in xenon can be resolved into $np[2\frac{1}{2}]_2$, $np[1\frac{1}{2}]_2$, and $np[1\frac{1}{2}]_0$ components which cannot be resolved for the higher n levels. In the first series in krypton (Fig. 5), a few of the p states are barely resolved into two peaks, presumably a blended line containing $[2\frac{1}{2}]_2$ and $[1\frac{1}{2}]_2$ and the slightly resolved $[1\frac{1}{2}]_0$. The p' and f' autoionizing series in xenon (Fig. 4) are largely obscured by ionization due to three-photon resonance with the $5d[1\frac{1}{2}]_1$ level. The corresponding krypton spectrum (Fig. 6) represents a more fortunate case free of interference from three-photon resonances.

Each series was fit to the standard Rydberg formula $E_n = V_{IP} - R/(n - \delta)^2$ using a least-squares-fitting procedure, E_n is the measured energy of the Rydberg peak, V_{IP} is the ionization limit to which the series converges, n is the principal quantum number, δ is the quantum defect, and R is the Rydberg constant for the atom, $R_{Xe} = 109736.86$ and $R_{Kr} = 109736.60$ cm^{-1} . The results are tabulated in Tables I–VI. State energies are given in vacuum wave numbers.

In the p series in xenon, where the lower members are resolved but merge at higher n , fits were performed for each of the series of three resolved components, and a fourth fit was done for the unresolved members. In krypton, in which the lower members of the p series are partially resolved into two components, the quantum defects of the few, totally unresolved members agree with those of the one series of split components and were included in that fitting. The few xenon p' members have only $n = 10$ and 11 resolved, and so are insufficient in number to be fit to a Rydberg series. The higher members of the xenon f series yield a strongly varying quantum defect, so only the $n = 11$ – 17 members were used in the fitting procedure.

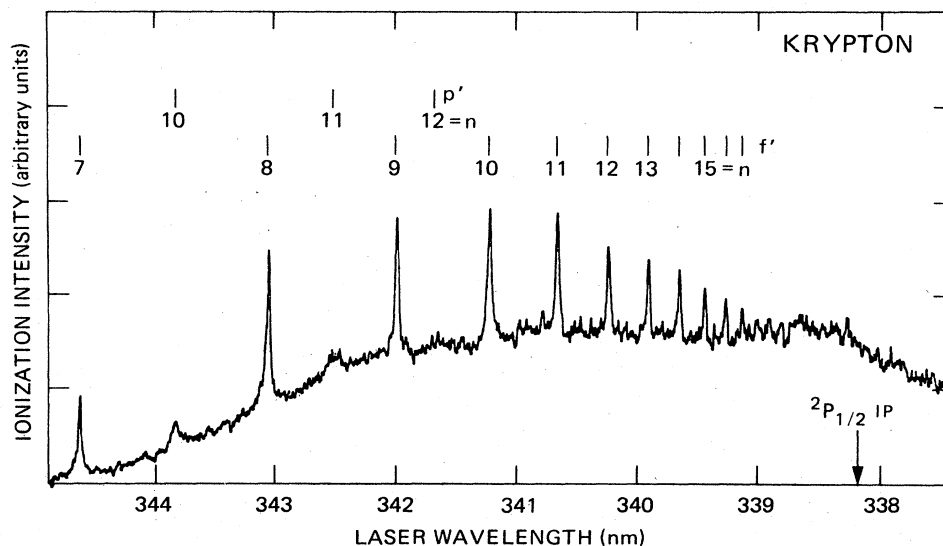


FIG. 6. The np' and nf' autoionizing series in krypton. The position of the $2P_{1/2}$ ionization limit is indicated.

TABLE I. The measured energy levels in cm^{-1} of the xenon nf series.

n	E observed	E calculated	n	E observed	E calculated
11	96 921	96 921	20	97 559	97 560
12	97 068	97 068	21	97 586	97 586
13	97 182	97 182	22	97 610	97 608
14	97 274	97 272	23	97 628	97 628
15	97 345	97 345	24	97 644	97 645
16	97 404	97 405	25	97 661	97 660
17	97 454	97 454	26	97 675	97 673
18	97 493	97 495	27	97 686	97 685
19	97 530	97 530			

The quantum defects and ionization potentials obtained from the fitting procedure are given in Table VI. With the exception of the krypton f' series, all series yield ionization potentials within a few cm^{-1} of the established values. It is unclear why the krypton f' series yields an aberrant result for the ionization potential, particularly because its defect is in good agreement with those calculated from some known f' sublevels, and since the concurrent p' series yields an acceptable V_{IP} . However, since the V_{IP} determined from the p' series has a large uncertainty, it may be that these series have some systematic shift to higher energy. The most satisfactory fit to a lower series in xenon is that for the $p[\frac{1}{2}]_0$ levels which yields a V_{IP} of $97\,831.8 \pm 1 \text{ cm}^{-1}$ which is still displaced slightly from the standard value of $97\,833.81$.⁶ The f' series in xenon yields the ${}^2P_{1/2}$ V_{IP} of $108\,371 \pm 2 \text{ cm}^{-1}$, in excellent agreement with the literature value.¹² The best fit for the lower V_{IP} in krypton is also from the $p[\frac{1}{2}]_0$ series giving $112\,915 \pm 2 \text{ cm}^{-1}$ in excellent agreement with the literature.¹²

Several comments regarding these spectra are appropriate. The relative intensities of the p and f series when excited from a metastable beam have attracted scrutiny.

The appearance of strong s - f transitions in xenon is well known and is explained by configuration mixing of $5d$ character into the $6s$ levels. Why the p series should appear so much more weakly has been a matter of speculation. Stebbings *et al.*⁴ have invoked perturbation of the p series by lower members of the p' series as a possible explanation. Knight and Wang⁶ have rejected this explanation in favor of one involving destructive interference of excitation pathways from the configuration-mixed metastable state.

We note here that in our spectra, obtained from direct, four-photon excitation without an intermediate state, the p resonances are also much weaker than the f resonances. In fact, this is true in each series in xenon and krypton. Additionally, we have scanned the ${}^2P_{3/2}$ series in xenon using a different laser with a slightly more narrow bandwidth and lower output power. In this spectrum (not presented here), the p transitions are markedly weaker relative to the f transitions than shown in Fig. 2. In our experiment, at least, this might imply that a much lower photoionization cross section for the p states determines the intensity difference. If the photoionization rate of the f states saturates, one would then expect an increase in the

TABLE II. The measured energy levels in cm^{-1} of the xenon np series.

n	$np[2\frac{1}{2}]_2$		$np[1\frac{1}{2}]_2$		$np[\frac{1}{2}]_0$	
	E observed	E calculated	E observed	E calculated	E observed	E calculated
14	96 832	96 831	96 841	96 840	96 855	96 854
15	96 997	96 998	97 005	97 005	97 015	97 016
16	97 126	97 127	97 130	97 132	97 140	97 140
17	97 228	97 228	97 232	97 232	97 239	97 238
18	97 309	97 309	97 313	97 312	97 317	97 317
19	97 375	97 374		97 379	97 381	97 381
20	97 428	97 428		97 432	97 434	97 434
Unresolved						
21			97 476	97 476		
22			97 513	97 514		
23			97 547	97 546		
24			97 574	97 574		
25			97 597	97 598		

TABLE III. The measured energy levels, in cm^{-1} , of the xenon nf' and np' series. The np' series cannot be fit to a Rydberg formula: $2 = np'[2\frac{1}{2}]_2$, $0 = np'[\frac{1}{2}]_0$.

nf'			np'	
n	E observed	E calculated	n	E observed
4	101 430	101 429	10_2	105 742
5	103 931	103 933	10_0	105 773
6	105 283	105 291	11_2	106 397
7	106 112	106 110	11_0	106 417
8		106 640	12	
9	107 001	107 004	13	107 032
10	107 270	107 264	14	107 384
11	107 452	107 456		

TABLE IV. The measured energy levels, in cm^{-1} , of the krypton nf and np series. The lower members of the p series are partly resolved into two series, probably $np[2\frac{1}{2}]_2 + np[1\frac{1}{2}]_2$ and $np[\frac{1}{2}]_0$.

n	nf		$np[2\frac{1}{2}]_2 + np[1\frac{1}{2}]_2$		$np[\frac{1}{2}]_0$	
	E observed	E calculated	E observed	E calculated	E observed	E calculated
10	111 814	111 813				
11	112 004	112 004				
12	112 146	112 149				
13	112 263	112 262			111 914	111 914
14	112 352	112 352	112 070	112 071	112 080	112 080
15	112 424	112 424	112 200	112 201	112 208	112 209
16	112 483	112 483	112 305	112 303	112 310	112 309
17				112 385		
18			112 453	112 451		
19			112 503	112 506		

TABLE V. The measured energy levels, in cm^{-1} , of the krypton nf' and np' series.

n	nf'		np'	
	E observed	E calculated	E observed	E calculated
7	116043	116043		
8	116572	116572		
9	116932	116934		
10	117192	117193	116321	116323
11	117381	117385	116767	116758
12	117536	117530	117054	117063
13	117644	117644	117306	117284
14	117741	117733	117453	117451
15	117800	117806		
16	117868	117865		
17	117917	117914		
18	117948	117955		

TABLE VI. The results of the least-squares fit of the data to Rydberg series and comparison to established values. Tabulated uncertainties are least-squares estimates of deviation from best values.

	This work			Literature		Refs.
	V_{IP} (cm^{-1})	δ		V_{IP} (cm^{-1})	δ	
Xenon						
nf	$97\,835.5 \pm 1$	0.055	$nf[\frac{3}{2}]_1$	97 833.81	0.0560	6
$np[2\frac{1}{2}]_2$	$97\,834.0 \pm 1$	3.52	$np[\frac{1}{2}]_1$	97 833.81	3.596	6
$np[1\frac{1}{2}]_2$	$97\,833.5 \pm 2$	3.47				
$np[\frac{1}{2}]_0$	$97\,831.8 \pm 1$	3.42				
np (unresolved)	$97\,837 \pm 3$	3.48				
nf'	$108\,371 \pm 2$	0.011		108 371.4		12
			$5f'$		0.028	3
		3.54;	$8p'[\frac{3}{2}]_1$		3.59	3
np'		3.50	$8p'[\frac{1}{2}]_1$		3.55	3
Krypton						
nf	$112\,911 \pm 5$	0.016		112 915.2		12
$np[2\frac{1}{2}]_2 + np[\frac{1}{2}]_2$	$112\,913 \pm 4$	2.58				
$np[\frac{1}{2}]_0$	$112\,915 \pm 2$	2.50				
nf'	$118\,295 \pm 2$	0.021		118 284.7		12
np'	$118\,284 \pm 15$	2.51				

intensities of the p states relative to the f states at a higher power level. Additional attempts to study the power dependence of the intensities have not been undertaken.

The mechanisms by which the Rydberg atoms ionize in our experiments have not been systematically studied. In addition to photoionization, collisional or associative ionization, or field ionization due to the collection potential in the cell might be expected to play a role. However, the collection field in the vicinity of the focal region in the cell is only on the order of a few hundred volts per cm. Therefore, no field ionization of our observed Rydberg states would be expected. The intensity of the f' series in krypton was observed to have a stronger pressure dependence than that of the p' series. This effect is presently being studied in detail and will be the subject of a separate report. No other effects in the intensities of the higher n members of the series relative to that of the lower members have been observed on changing the pressure or field strength.

The high-order process used here to observe the Rydberg series can only be achieved at high ($\sim 10^{10}$ W/cm²) power densities. Under such conditions, levels which are nearly resonant with the third photon can be expected to give an ac Stark effect in the observation of the Rydberg levels. The resultant shift and broadening observed in such a spectrum may limit the resolution and accuracy of measured peak locations in such an experiment. Thus, it would not be expected that this technique could be extended to high-resolution determinations. It does not ap-

pear that the apparent shift of the krypton autoionizing series could be due to such an effect. Rough calculations have been done for a worst-case situation as in the xenon autoionizing series, where a three-photon resonance to a $5d$ level obscures several members. The calculation indicates an ac Stark broadening of $2\text{--}5$ cm⁻¹ for the nearest observed members under our conditions. Overall, we seem to be able to obtain quite satisfactory results from the experiments.

It should also be noted that in the case of excitation of the autoionizing series in both xenon and krypton, third-harmonic light may play a role in the excitation. This is because three photons reach regions lying just above one-photon allowed resonances where the medium is negatively dispersive. It is known that where a third-harmonic excitation mechanism exists, it can totally dominate the spectrum.^{10,13} The excitation mechanism then involves one third-harmonic photon plus one laser photon. In such a case, two-photon selection rules apply, and $J=4$ levels will not be observed from the rare-gas ground state. However, our laser resolution does not allow observation of separate $f[K]_J$ sublevels. The p sublevels observed are allowed both by two-photon and four-photon selection rules. No attempt was made to directly search for third-harmonic light.

These experiments provide a striking reminder that "nonresonant" ionization into a continuum where autoionizing resonances are imbedded can have a considerable wavelength dependent structure. This situation could give rise to complicated MPI spectra in atoms and mole-

cules when the ion yield is due to a convolution of resonant enhancement at an intermediate level and in the ionization step.

CONCLUSION

We have shown that direct, four-photon excitation with no resonant intermediate states can be profitably used to probe high Rydberg and autoionizing states in xenon and krypton. Exploitation of selection rules in multiphoton excitation allows the observation of many p and f states. In this way, we have identified members of the $p[2\frac{1}{2}]_2$, $p[1\frac{1}{2}]_2$, and $p[\frac{1}{2}]_0$ series in xenon and have extended earlier observations on autoionizing series in xenon and krypton.

ACKNOWLEDGMENTS

We are grateful to R. N. Compton and P. Lambropoulos for their comments. One of us (P.R.B.) would like to thank the Chemical Physics Section, Oak Ridge National Laboratory, and the Oak Ridge Associated Universities for support. One of us (J.A.D.S.) wishes to express his appreciation to the Research Center of Crete for its hospitality. This research is sponsored by the Office of Health and Environmental Research, U.S. Department of Energy under Contract No. DE-AC05-84OR21400 with Martin Marietta Energy Systems, Inc. We also wish to express our gratitude for support received under a NATO collaborative research grant.

*Also at Department of Chemistry, Yale University, New Haven, CT 06520.

¹K. Yoshino, *J. Opt. Soc. Am.* **60**, 1220 (1970); K. Yoshino and Y. Tanaka, *ibid.* **69**, 159 (1978); K. Yoshino and D. E. Freeman, *J. Opt. Soc. Am. B* **2**, 1268 (1985); K. D. Bonin, T. J. McIlrath, and K. Yoshino, *ibid.* **2**, 1275 (1985).

²R. F. Stebbings and F. B. Dunning, *Phys. Rev. A* **8**, 665 (1973); F. B. Dunning and R. F. Stebbings, *ibid.* **9**, 2378 (1974).

³R. D. Rundel, F. B. Dunning, H. C. Goldwire, and R. F. Stebbings, *J. Opt. Soc. Am.* **65**, 628 (1975).

⁴R. F. Stebbings, C. J. Latimer, W. P. West, F. B. Dunning and T. B. Cook, *Phys. Rev. A* **12**, 1453 (1975).

⁵J. P. Grandin and X. Husson, *J. Phys. B* **14**, 433 (1981).

⁶R. D. Knight and L.-G. Wang, *J. Opt. Soc. Am. B* **2**, 1084

(1985).

⁷M. Thekaekara and G. H. Dieke, *Phys. Rev.* **109**, 2029 (1958).

⁸R. F. King and C. J. Latimer, *J. Opt. Soc. Am.* **72**, 306 (1982).

⁹K. Aron and P. M. Johnson, *J. Chem. Phys.* **67**, 5099 (1977).

¹⁰R. N. Compton and J. C. Miller, *J. Opt. Soc. Am. B* **2**, 355 (1985).

¹¹P. Gangopadhyay, X. Tang, P. Lambropoulos, and R. Shakeshaft, *Phys. Rev. A* **34**, 2998 (1986).

¹²C. E. Moore, *Atomic Energy Levels*, Natl. Bur. Stand. (U.S.) Circ. No. 467 (U.S. GPO, Washington, D.C., 1952), Vol. II, p. 169; *ibid.* (U.S. GPO, Washington, D.C., 1958), Vol. III, p. 113.

¹³W. R. Garrett, W. R. Ferrell, M. G. Payne, and J. C. Miller, *Phys. Rev. A* **34**, 1165 (1986).